

Considerations around the SARS-CoV-2 Spike Protein with particular attention to COVID-19 brain infection and neurological symptoms

Kambiz Hassanzadeh, Helena Perez Pena, Jessica Dragotto, Lucia Buccarello,
Federico Iorio, Stefano Pieraccini, Giulio Sancini, and Marco Feligioni

ACS Chem. Neurosci., **Just Accepted Manuscript** • DOI: 10.1021/acchemneuro.0c00373 • Publication Date (Web): 06 Jul 2020

Downloaded from pubs.acs.org on July 18, 2020

Just Accepted

“Just Accepted” manuscripts have been peer-reviewed and accepted for publication. They are posted online prior to technical editing, formatting for publication and author proofing. The American Chemical Society provides “Just Accepted” as a service to the research community to expedite the dissemination of scientific material as soon as possible after acceptance. “Just Accepted” manuscripts appear in full in PDF format accompanied by an HTML abstract. “Just Accepted” manuscripts have been fully peer reviewed, but should not be considered the official version of record. They are citable by the Digital Object Identifier (DOI®). “Just Accepted” is an optional service offered to authors. Therefore, the “Just Accepted” Web site may not include all articles that will be published in the journal. After a manuscript is technically edited and formatted, it will be removed from the “Just Accepted” Web site and published as an ASAP article. Note that technical editing may introduce minor changes to the manuscript text and/or graphics which could affect content, and all legal disclaimers and ethical guidelines that apply to the journal pertain. ACS cannot be held responsible for errors or consequences arising from the use of information contained in these “Just Accepted” manuscripts.

Considerations around the SARS-CoV-2 Spike Protein with particular attention to COVID-19 brain infection and neurological symptoms

Kambiz Hassanzadeh^{1,2}, Helena Perez Pena³, Jessica Dragotto¹, Lucia Buccarello¹, Federico Iorio¹, Stefano Pieraccini^{3,4}, Giulio Sancini^{5} and Marco Feligioni^{*1,6}**

1. Laboratory of Neuronal Cell Signaling, EBRI Rita Levi-Montalcini Foundation, Rome 00161, Italy.
2. Cellular and Molecular Research Center, Research Institute for Health Development, Kurdistan University of Medical Sciences, Sanandaj, Iran. Postal Code: 66177-13446,
3. Department of Chemistry and National Inter-University Consortium for Materials Science and Technology -INSTM- UdR Milano, University of Milan, Milan, 20133, Italy.
4. Institute of Science and Chemical Technology "Giulio Natta", Milan, 20133, Italy.
5. Human Physiology Lab., School of Medicine and Surgery, University of Milano-Bicocca, Via Cadore 48, 20900, Monza, Italy.
6. Department of Neurorehabilitation Sciences, Casa di Cura del Policlinico, Milan 20144, Italy.

Running Title: SARS-CoV-2 Spike Protein and brain infection

** Co-last author: Giulio Sancini

*Corresponding author:

Marco Feligioni, PhD

European Brain Research Institute (EBRI) Rita Levi Montalcini Foundation,

Viale Regina Elena 295, 00161 Rome, Italy

Phone: +39 06 49 255 255 , Fax: +39 06 49 255 255

e-mail: m.feligioni@ebri.it

Abstract

Spike protein (S protein) is the virus 'key' to infect cells being able to strongly bind to the human angiotensin-converting enzyme2 (ACE2), as it has been reported. In fact, Spike structure and function is known to be highly important for cell infection as well as entering the brain. Growing evidence indicates that different types of coronaviruses not only affect the respiratory system, but they might also invade the central nervous system (CNS). However, very few evidence have been so far reported on the presence of COVID-19 in the brain and the potential exploitation, by this virus, of lung to brain axis to reach neurons has not completely understood. In this article we assessed the SARS-CoV and SARS-CoV-2 Spike protein sequence, structure and electrostatic potential using computational approaches. Our results showed that the S proteins of SARS-CoV-2 and SARS-CoV are highly similar, sharing a sequence identity of 77%. In addition, we found that the SARS-CoV-2 S protein is slightly more positively charged than that of SARS-CoV since it contains four more positively charged residues and five less negatively charged residues which may lead to an increased affinity to bind to negatively charged regions of other molecules through non-specific and specific interactions. Analyzing of the S protein binds to the host ACE2 receptor showed a 30% higher binding energy for SARS-CoV-2 than the SARS-CoV S protein. These results might be useful for understanding the mechanism of cell entry, blood brain barrier crossing and clinical features related to the CNS infection by SARS-CoV-2.

Key Words: ACE2, Brain, COVID-19, Spike Protein

Introduction

The crucial step in the viral infection is the process of viral entry into the host cells and understanding this mechanism is important for exploring the effective therapeutic agents in the treatment of viral infection. Endocytic pathway including endosome and lysosome and the autophagy process in viral entry has attracted considerable attention as therapeutic targets in combating diseases caused by virus in the last decade¹.

The clathrin-dependent endocytotic/exocytotic has been reported the main pathway for some viruses enter host cells such as Hepatitis C virus, Tick-borne encephalitis virus and Zika virus which enter the astrocytes and induce neuro-infection by endocytosis^{2,3}. Whether SARS-Co-V2 infects neuronal system by this mechanism has yet to be elucidated. Having in mind that other type of coronavirus, swine hemagglutinating encephalomyelitis virus (HEV), employs endocytosis for its trans-synaptic transfer⁴.

From a molecular point of view, computational modeling studies highlighted the huge similarity between SARS-CoV-2 with the original SARS-CoV especially in the 3-D structures of the receptor-binding domain of the Spike proteins (S). Several lines of evidence focused on Spike protein as a main tool of the virus to infect cells being able to strongly bind to the Angiotensin converting enzyme 2 (ACE2)^{5,6}.

The Spike protein is a homotrimer that protrudes from the viral membrane and contains, in each of its monomers, a Receptor Binding Domain (RBD) through which this viral protein directly interacts with the ACE2 receptor located on the surface of many host cells⁷⁻¹⁰.

ACE2 is an enzyme attached to the outer surface (cell membranes) of cells in the lungs, arteries, heart, kidney, intestines and brain¹¹. The ACE2 which is expressed in the brain,

1
2
3 mainly existing in the brain stem and in the regions involved in cardiovascular function and
4
5 central regulation of blood pressure including subfornical organ, nucleus of the tractus
6
7 solitarius, paraventricular nucleus, and rostral ventrolateral medulla^{12,13}.
8
9

10 In a previous study, Wrapp et al. reported that SARS-CoV-2 S protein exhibits higher
11
12 binding affinity to the ACE2 receptor than that of the SARS-CoV¹⁴.
13

14 SARS-CoV and SARS-CoV-2 share about 96% nucleotide sequence identities, suggesting
15
16 that SARS-CoV- 2 might have emerged from a bat SARS-like coronavirus. Therefore, in
17
18 this study we investigated the differences between the sequence, structure and
19
20 electrostatic potential of SARS-CoV-2 and SARS-CoV Spike proteins both in their open
21
22 and close conformations using computational approaches and discuss how these
23
24 divergences may make this new virus highly infectious to the human cells and organs with
25
26 particular attention to brain infection and neurologic symptoms in patients with COVID-19.
27
28 In fact, although the most prevalent symptom that leads COVID-19 patients to the intensive
29
30 care units, is the heavy respiratory complications, some patients also showed neurologic
31
32 signs which have been described in three categories: central nervous system (CNS)
33
34 symptoms or diseases (headache, dizziness, impaired consciousness, ataxia, acute
35
36 cerebrovascular disease, and epilepsy), peripheral nervous system (PNS) symptoms
37
38 (hypogeusia, hyposmia and neuralgia), and skeletal muscular symptoms ^{15,16}. Recently,
39
40 more serious complications including, acute encephalopathy¹⁷ and acute hemorrhagic
41
42 necrotizing encephalopathy (ANE)¹⁸ have been reported in case report studies. ANE is a
43
44 rare complication of viral infections such as influenza and has been related to remarkable
45
46 increase in intracranial cytokine, which leads to BBB breakdown¹⁹.
47
48
49
50
51
52
53
54
55
56
57
58
59
60

1
2
3 There is no evidence regarding the entry of SARS-CoV-2 to the brain to date neither in
4 animal nor human studies. Indeed, several papers reported the presence of SARS-CoV in
5 the central nervous system (CNS) especially found in CSF like in the report in which the
6 status epilepticus of a patient was associated with SARS²⁰ and others reports in which
7 demyelinating brain pathology have been associated to coronaviruses infection ²¹. Besides,
8 some clinical studies performed on patients affected by SARS-CoV have identified the
9 presence of virus particles in the brain, mainly localized in the neurons ²²⁻²⁴.

10
11 Therefore, in this article we also discuss the possible pathological interaction between brain
12 and lung, CNS infection and relevant clinical futures in patients with COVID-19 based on
13 our current knowledge.

24 **Results and discussion**

25
26 The results of sequence alignment, shows that the sequences of the S proteins of SARS-
27 CoV-2 and SARS-CoV are highly similar, sharing a sequence identity of 77%. Nonetheless,
28 some divergences can be observed in the sequence (Figure 1 and supplementary data).
29 These divergences have been examined in a previous study by Jaimes et al. who
30 represented in the 3-dimesional (3D) structures of the proteins²⁵. Moreover, Baig et al.
31 suggest that these differences may be related to the higher binding affinity of SARS-CoV-
32 2 S protein to the host ACE2 receptor²⁶.

33
34 More recently, Robson indicated that all human SARS coronaviruses (and indeed the spike
35 proteins of many other related coronaviruses) seem similar in general conformation, and
36 the variations observed in experimental structures are probably more to do with
37 crystallization or other preparation methods²⁷.

1
2
3 Our findings reveal that, the SARS-CoV-2 S protein is slightly more positively charged than
4 that of SARS-CoV since it contains four more positively charged residues and five less
5 negatively charged residues (Table 1). Even if the difference in charge between SARS-
6 CoV-2 and SARS-CoV S proteins is rather small, this effect can be amplified by the high
7 number of S proteins that are present on a virus particle. This difference in charge between
8 SARS-CoV-2 and SARS-CoV S proteins can have a significant impact in cell adhesion and
9 crossing the blood brain barrier ^{28,29} which will be discussed more in detail, later in this
10 article.
11
12

13
14 A two-step process takes place when the S proteins interact with other proteins, such as
15 when the S protein binds to the human ACE2 receptor, to establish a final protein-protein
16 association. (1) The first step is dominated by electrostatic forces that lead the formation of
17 an ensemble of transient and non-specific encounter complexes³⁰. In this step, the S
18 protein would be found in the closed conformation. (2) A structural rearrangement takes
19 place in the protein and the three S protein RBDs open up to expose their binding interface
20 to form a well-defined complex, which is stabilized not only by electrostatic forces, but also
21 by polar (salt-bridge and hydrogen bond) and non-polar interactions (π -stack, π -anion, and
22 short-range hydrophobic interactions)^{7,30}. Taking this into account, the electrostatic
23 potential of both SARS-CoV-2 and SARS-CoV S protein surfaces, both in the open and
24 close conformations, has been calculated in this study (see Figure 2), also focusing in their
25 RBDs, in order to analyze the differences in the ability of SARS-CoV-2 and SARS-CoV to
26 bind to other molecules within the human body according to their electrostatic properties,
27 and thus, their capacity to enter human cells.
28
29
30
31
32
33
34
35
36
37
38
39
40
41
42
43
44
45
46
47
48
49
50
51
52
53
54
55
56
57
58
59
60

1
2
3 Several structures of S proteins could be found in the Protein Data Bank (PDB), but in all
4 of them were present not resolved segments. In order to calculate and map a protein
5 electrostatic potential a complete structure is needed, therefore complete 3D structures of
6 SARS-CoV-2 and SARS-CoV protein S, both in the open and close conformation, were
7 modelled using homology modelling techniques.
8
9

10 Having modelled SARS-CoV-2 and SARS-CoV S protein structures, both structures in the
11 close state conformation were superimposed with 1.236 Å Root-Mean-Square Deviation
12 (RMSD) over 427 aligned C α positions. In this way, the structure of both proteins was
13 compared showing a high structure similarity.
14

15 Afterwards, macromolecular electrostatic calculations of the models were performed. In
16 other studies, differences in the RBD:ACE2 interfaces between SARS-CoV-2 and SARS-
17 CoV S protein at a structural level have already been described in detail and have been
18 linked to SARS-CoV-2 higher binding affinity. Herein, these interfaces have been analyzed
19 at the electrostatic potential level (see Figure 3, Figure 4).
20
21
22

23 Recently, in a report published in Nature, Lan et al., identified residues in the SARS-CoV-2
24 RBD that are essential for ACE2 binding, the majority of which either are highly
25 conserved or share similar side chain properties with those in the SARS-CoV RBD. They
26 believe that similarity in structure and sequence strongly indicate convergent evolution
27 between the SARS-CoV-2 and SARS-CoV RBDs for improved binding to ACE2³¹.
28
29
30
31
32

33 In Figure 2, the electrostatic potentials of SARS-CoV-2 and SARS-CoV S protein (top side)
34 are compared, showing that the SARS-CoV-2 S protein surface exhibits a more positive
35 electrostatic potential than that of SARS-CoV. This same electrostatic potential difference
36 can also be seen in the binding interface of their RBDs (Figure 3). Thus, despite presenting
37
38
39
40
41
42
43
44
45
46
47
48
49
50
51
52
53
54
55
56
57
58
59
60

1
2
3 a high sequence and structural similarity, SARS-CoV-2 and SARS-CoV S proteins have
4 different electrostatic properties. This difference can have an effect on the capacity of the
5 virus to adhere to other molecules. On the other side, human ACE2 binding interface tends
6 to have a predominantly negative electrostatic potential (Figure 4) and, therefore, will
7 interact more strongly with the SARS-CoV-2 S protein both in the open and close
8 conformations.
9

10 Comparing SARS-CoV-2 and SARS-CoV S protein sequences, 3D structures and
11 electrostatic potentials, reveals that both proteins have a conserved sequence and
12 structural features, but different electrostatic characteristics in both their external surface
13 and their host-interaction interfaces. As previously described, the SARS-CoV-2 S protein
14 is slightly more positively charged in these regions than that of SARS-CoV, which will lead
15 to an increased affinity to bind to negatively charged regions of other molecules through
16 non-specific and specific interactions.
17

18 Moreover, some differences in the amino acidic content of the S protein in the RBD-ACE2
19 interface can lead to the establishment of more specific interactions with the host receptors.
20 Hence, SARS-CoV-2 is more likely to establish interactions with different targets across the
21 human body than SARS-CoV both through non-specific and specific interactions. All this,
22 ultimately, can increase the capacity of SARS-CoV-2 to enter human cells and binding to
23 the negatives charge barriers such as BBB³² with respect to SARS-CoV.
24

25 In the last months, S protein structure and electrostatic properties have been the object of
26 much investigation. Previous computer-based experiments have also noted that the SARS-
27 CoV-2 RBD exhibits a more positive electrostatic potential than the SARS-CoV RBD^{31,33–35}
28 and that the electrostatic potential has a particularly important role in the high infection rate
29
30
31
32
33
34
35
36
37
38
39
40
41
42
43
44
45
46
47
48
49
50
51
52
53
54
55
56
57
58
59
60

1
2
3 of SARS-CoV-2. In agreement with our results, it has previously been observed that SARS-
4
5 CoV-2 binds with a higher affinity to the human ACE2 receptor than SARS-CoV³³. This was
6
7 also attributed to the enhanced electrostatic interactions between SARS-CoV-2 and ACE2
8
9 due to the SARS-CoV-2 RBD having greater electrostatic complementarity with the binding
10
11 domain of ACE2 than the SARS-CoV RBD³³. In particular, it has been reported that the
12
13 increased positive electrostatic potential of the SARS-CoV-2 binding surface is mainly due
14
15 to an essential mutation of the hydrophobic residue Val404, present in SARS-CoV, to the
16
17 positively charged residue Lys417 in SARS-CoV-2^{31,34}.

18
19
20
21
22 Amin et al. also identified a complementary negative electrostatic potential on the surface
23
24 of the binding site of ACE2³³.

25
26
27 Taking advantage of our previous experience dealing with nanoparticles (NPs) specifically
28
29 tailored to cross the blood brain barrier (BBB) and target the brain tissue we can speculate
30
31 the potential strategies of COVID-19 to enter into the brain. Indeed, the dimension and the
32
33 surface properties of the COVID-19 is similar, in terms of adhesion and cell membrane
34
35 crossing abilities, to those shown by the nanoparticles specifically designed for BBB
36
37 crossing^{29,36}. So the parallelism between COVID-19 and the strategies adopted to let
38
39 nanoparticles cross the BBB can be useful to hypothesized the ways used by the virus to
40
41 enter into the brain. Therefore, an increase of the number of the positive amino acids of the
42
43 COVID-19 envelope might increase in a significant manner the adhesion properties of the
44
45 COVID-19 crossing the BBB and entering the brain.

46
47
48 In order to quantify the difference in the binding affinity of the two complexes (SARS-CoV-
49
50 2:ACE2 and SARS-CoV:ACE2), their binding free energy was calculated. The results
51
52 showed that SARS-CoV-2 S protein binds to the host ACE2 receptor with a 30% higher
53
54
55
56
57
58
59
60

1
2
3 binding energy than the SARS-CoV S protein. It has also been observed that the
4 electrostatic contribution to the total binding free energy is the dominant term in the SARS-
5 CoV-2:ACE2 interaction. Hence, this data supports the qualitative analysis of the
6 electrostatic potential of the structures presented above and the quantitative data shown in
7 previous studies.
8
9

10
11
12 According to the bioinformatics data regarding the possible interaction between virus Spike
13 protein and ACE2 protein, it is suggested that SARS-CoV-2 is probable to adhere with
14 higher efficiency to the cells through a non-specific interactions which have a major impact
15 on cell adhesion²⁸ due to 1) SARS-CoV-2 electrostatic properties and, 2) binds with higher
16 affinity to the host ACE2 receptor through specific interactions. In fact, our findings revealed
17 that the Spike protein of SARS-CoV-2 binds to the host ACE2 receptor with a significant
18 higher binding energy than the SARS-CoV S protein, indicating the electrostatic
19 contribution to the total binding free energy is the dominant term in the SARS-CoV-2:ACE2
20 interaction.
21
22

23
24
25 As previously described, Spike protein and ACE2 represents the key, but not the exclusive,
26 site of entry of the virus into the cell, thus non-ACE2 pathways for virus infection of neural
27 cells also cannot be excluded³⁷. Whether Covid-19 infects neurons, astroglial cells and
28 enters astrocytes by endocytosis remains to be studied. Overall, considering the
29 computational assay that have been performed in this study we suggest that Spike protein
30 dependent pathway is thought to be more important than clathrin-dependent endocytosis
31 for cell entry and BBB crossing. Therefore, Spike dependent pathway should be taken into
32 account in therapeutic strategies for specific antibodies or vaccine production research.
33
34
35
36
37
38
39
40
41
42
43
44
45
46
47
48
49
50
51
52
53
54
55
56
57
58
59
60

1
2
3 Regardless of how the virus enters the brain, there are some CNS complications in patients
4 with COVID-19 that should be taken into consideration.
5

6
7 The presence of the virus in the brain stem may affect chemo-sensing neural cells related
8 to the respiration as well as respiratory center neurons thus damaging the lung ventilatory
9 function³⁷.
10
11

12
13 It has been shown that SARS-CoV downregulate ACE2 protein expression in a replication
14 dependent manner³⁸. Supporting these finding, it has been revealed that SARS-CoV
15 infections and the Spike protein of the SARS-CoV reduced the ACE2 expression and the
16 injection of SARS-CoV Spike into mice worsened acute lung failure in vivo, which was
17 attenuated by blocking the renin-angiotensin pathway³⁹.
18
19

20
21 Considering the high similarity of SARS-CoV and COVID-19, and higher binding energy of
22 COVID-19 than the SARS-CoV S protein to bind the ACE2, it has been hypothesized that
23 SARS-CoV-2 also can downregulate ACE2 in different organs including brain^{40,41}. This
24 downregulation might be a part of this complicated story; inhibition of ACE2 activity,
25 reduces the sensitivity of the baroreceptor reflex control of heart rate as well as increase in
26 sympathetic tone, eventually resulting in the blood pressure elevation and cardiac
27 dysfunction. On the other hand, increasing of inflammatory cytokines during lung injury,
28 hypoxemia and elevation of sympathetic tone through ACE2 downregulation leads to CNS
29 hyper-activation which might play a crucial role in etiopathogenesis of neurogenic
30 pulmonary edema (NPE)⁴², a life-threatening complication following a neurologic insult⁴³,
31 and finally deteriorating the respiratory and cardiovascular complications in these patients
32 (see figure 5).
33
34
35
36
37
38
39
40
41
42
43
44
45
46
47
48
49
50
51
52
53
54
55
56
57
58
59
60

1
2
3 Supporting the idea of brain infection, more recently, in a case report one patient was
4 described with no past medical history showed frequent seizures probably due to COVID-
5 19 infection⁴⁴. Several mechanisms for the etiology of seizure have been taken into
6 consideration, including the direct infiltration of brain tissue, production of toxins by the virus
7 or increasing of inflammatory cytokines by the brain⁴⁵. Recently, It has been reported that
8 COVID-19 initiates the inflammatory cascade and as a result, releases inflammatory
9 cytokines⁴⁶ which is called cytokine storm syndrome⁴⁷. Consecutively, these cytokines can
10 drive neuronal hyper-excitability via activation of glutamate receptors and play a role in the
11 development of acute seizures^{48–50}.

12
13 In addition, in a case report study, it was presented a case of self-limited encephalitic
14 associate with SARS-CoV-2. The authors suggested that with the clearance of virus and
15 the use of mannitol, the CSF pressure might gradually decrease and the patient's
16 consciousness will improve⁵¹.

17
18 In a recent study, neurologic features in severe Covid-19 patients who admitted to the
19 hospital has been reported. Magnetic resonance imaging (MRI) of the brain was performed
20 in 13 patients in this evaluation. Although these patients did not have focal signs that
21 suggested stroke, they underwent MRI because of unexplained encephalopathic features.
22 Two of 13 patients who underwent brain MRI showed single acute ischemic strokes.
23 Authors concluded that their data were not enough to recognize which of these features
24 were due to critical illness–related encephalopathy, cytokines, or the effect or withdrawal
25 of medication, and which features were directly due to SARS-CoV-2 infection.

26
27 Post-viral anosmia which is also named olfactory dysfunction^{52,53} and ageusia⁵⁴ are other
28 neurologic symptoms have been reported in patients with COVID-19. More recently in a
29
30
31
32
33
34
35
36
37
38
39
40
41
42
43
44
45
46
47
48
49
50

1
2
3 cross-sectional study in Iran on 10,069 cases, coincidence of COVID-19 epidemic and
4 olfactory dysfunction has been reported⁵⁵. In this context, recently, Lechien et al. reported
5 that olfactory and gustatory dysfunctions are prevalent in patients with mild-to-moderate
6 COVID-19 infection⁵⁶. Some mechanisms have been raised to explain this association
7 including 1) injury at the level of the neuro-epithelium of olfactory receptor cells in the nasal
8 roof or in the central olfactory processing system⁵⁵ 2) damage of the central olfactory routes
9 and other regions of the brain^{57–59} 3) inflammation or the possible damages to the nasal
10 epithelium cells that required for normal olfactory function⁶⁰. Therefore, both epithelial
11 damage and CNS involvement, have been reported as the possible causes; however, its
12 exact pathophysiology remains yet to be elucidated^{53,61}.

13
14
15
16
17
18
19
20
21
22
23
24
25
26 In accordance with the neurotrophic mechanism proposed by Baig et al.,¹⁰ which
27 hypothesizes the COVID-19 brain access via the transcribrial route, as documented for
28 other CNS targeting pathogens, we suppose a possible entry of the virus from the olfactory
29 bulb and, exploiting the blood microcirculation, the COVID-19 may have access to the
30 cerebral circulation and interact with ACE2 receptors expressed on neuronal cells.
31
32
33
34
35
36
37
38
39
40

41 **Conclusion**

42
43
44 Considering the neurological manifestations of patients with COVID-19 and in light of the
45 bioinformatics findings of this study indicating more positive charged spike protein structure
46 and higher binding free energy of the SARS-CoV-2:ACE2 interaction, it is expected that
47 COVID-19 possess higher efficiency than SARS-CoV to enter the cells and reaching the
48 brain. This neuro-invasive characteristic, should be taken into account in the basic and
49 clinical research as well as prioritization and individualization of therapeutic approach.
50
51
52
53
54
55
56
57
58
59
60

Methods:

Spike protein sequence alignment and analysis

The sequence alignment of the S protein of SARS-CoV-2 (UniProt ID P0DTC2) and SARS-CoV (UniProt ID P59594) was conducted in the webserver BLASTp⁶² using the Needleman-Wüncsh algorithm with the default substitution matrix (BLOSUM62)⁶³ (see Figure 1). For illustrative purposes, the resulting sequence alignment was downloaded as a text file from BLASTp and converted into an ALI format file in order to visualize and produce the sequence alignment images on the Molsoft Browser 3.9^{64,65}. In order to analyze the divergence in the amino acidic content of the S protein from SARS-CoV-2 and SARS-CoV, the number of each residue present in each protein sequence was counted using the “str_count“ function in RStudio 3.6.3 (Table1)⁶⁶.

Homology modeling and structure comparison

Homology models of the complete 3D structures of SARS-CoV-2 and SARS-CoV S protein, both in the open and close conformation, were built in the MODELLER 9.23⁶⁷ program by using a sequence alignment extracted from BLASTp⁶² and template structures obtained from the PDB⁶⁸ (Supplementary data). Homology models of SARS-CoV-2 and SARS-CoV S protein in the close conformation were superimposed using the structure comparison tool Match Maker in the software UCSF Chimera 1.14⁶⁹

Calculation of the electrostatic potential

Electrostatic potentials of the homology models were calculated using the program Adaptive Poisson-Boltzmann Solver (APBS)⁷⁰ and were displayed in PyMol 2.3.4⁷¹ as a

1
2
3 color-coded electrostatic potential molecular surface (Solvent-Excluded Surfaces (SESs))
4
5 by using the APBS 1.5 plugin ⁷² (see Figure 2).
6
7

8 **Binding free energy calculation**

9
10 In order to quantify the difference in the binding affinity of complexes SARS-CoV-2:ACE2
11 and SARS-CoV:ACE2, their binding free energy was calculated using the Molecular
12 Mechanics-Poisson Boltzmann Surface Area (MM-PBSA) approach⁷³ implemented in the
13 GROMACS-5.0.7 tool `g_mmpbsa`⁷⁴. MM-PBSA is a fully atomistic method for the
14 calculation of binding free energies that combines a molecular mechanics description of
15 the protein complex with a continuous solvent model. It is widely used to evaluate
16 interaction energies between proteins and biomolecules in general⁷⁵.
17
18
19
20
21
22
23
24
25
26

27 The structures of the SARS-CoV-2 S protein in complex with ACE2 receptor (PDB ID 6LZG)
28 and the SARS-CoV S protein in complex with ACE2 receptor (PDB ID 6ACG) were
29 subjected to geometry optimization in GROMACS-5.0.7 ⁷⁶ prior to the calculation. A relative
30 dielectric constant $\epsilon=80$ was used to model the water solvent while $\epsilon=2$ was used for the
31 protein in the solution of the Poisson-Boltzmann equation.
32
33
34
35
36
37
38
39
40
41
42
43
44
45

46 **Supporting Information**

47
48
49 Table of detailed sequence alignments used for homology modelling is available (PDF) as
50 supporting information.
51
52
53

54 **Author Contributions**

1
2
3 Kambiz Hassanzadeh: Designing, investigation and Writing the original draft; Helena Perez
4
5 Pena: Methodology, investigation, figures and tables preparation; Jessica Dragotto:
6
7 Prepared figures and writing the original draft; Lucia Buccarello: Revising the manuscript
8
9 critically for important intellectual content; Federico Iorio: Performed the literature search;
10
11 Stefano Pieraccini: Designing and methodology; Giulio Sancini: Co-supervision of project;
12
13 Marco Feligioni: Conceiving the idea, Designing the study and supervision of project, funds
14
15 . The manuscript was reviewed by all authors.
16
17
18
19

20 Conflict of interest

21
22
23 The authors declare that there is no conflict of interest
24
25

26 References

- 27
28
29 (1) Yang, N.; Shen, H.-M. Targeting the Endocytic Pathway and Autophagy Process as a Novel
30 Therapeutic Strategy in COVID-19. *Int. J. Biol. Sci.* **2020**, *16* (10), 1724–1731.
31 <https://doi.org/10.7150/ijbs.45498>.
32 (2) Jorgačevski, J.; Korva, M.; Potokar, M.; Lisjak, M.; Avšič-Županc, T.; Zorec, R. ZIKV Strains
33 Differentially Affect Survival of Human Fetal Astrocytes versus Neurons and Traffic of ZIKV-Laden
34 Endocytotic Compartments. *Sci. Rep.* **2019**, *9* (1), 1–14. [https://doi.org/10.1038/s41598-019-44559-](https://doi.org/10.1038/s41598-019-44559-8)
35 [8](https://doi.org/10.1038/s41598-019-44559-8).
36 (3) Zorec, R.; Županc, T. A.; Verkhatsky, A. Astrogliopathy in the Infectious Insults of the Brain.
37 *Neurosci. Lett.* **2019**, *689*, 56–62. <https://doi.org/10.1016/j.neulet.2018.08.003>.
38 (4) Li, Y.-C.; Bai, W.-Z.; Hirano, N.; Hayashida, T.; Taniguchi, T.; Sugita, Y.; Tohyama, K.; Hashikawa, T.
39 Neurotropic Virus Tracing Suggests a Membranous-Coating-Mediated Mechanism for Transsynaptic
40 Communication. *J. Comp. Neurol.* **2013**, *521* (1), 203–212. <https://doi.org/10.1002/cne.23171>.
41 (5) Li, F.; Li, W.; Farzan, M.; Harrison, S. C. Structure of SARS Coronavirus Spike Receptor-Binding
42 Domain Complexed with Receptor. *Science* **2005**, *309* (5742), 1864–1868.
43 <https://doi.org/10.1126/science.1116480>.
44 (6) Xu, X.; Chen, P.; Wang, J.; Feng, J.; Zhou, H.; Li, X.; Zhong, W.; Hao, P. Evolution of the Novel
45 Coronavirus from the Ongoing Wuhan Outbreak and Modeling of Its Spike Protein for Risk of
46 Human Transmission. *Sci. China Life Sci.* **2020**, *63* (3), 457–460. [https://doi.org/10.1007/s11427-](https://doi.org/10.1007/s11427-020-1637-5)
47 [020-1637-5](https://doi.org/10.1007/s11427-020-1637-5).
48 (7) Xie, L.; Sun, C.; Luo, C.; Zhang, Y.; Zhang, J.; Yang, J.; Chen, L.; Yang, J.; Li, J. SARS-CoV-2 and SARS-
49 CoV Spike-RBD Structure and Receptor Binding Comparison and Potential Implications on
50 Neutralizing Antibody and Vaccine Development. *bioRxiv* **2020**, No. December 2019,
51 2020.02.16.951723.
52
53
54
55
56
57
58
59
60

- 1
2
3 (8) Yan, R.; Zhang, Y.; Li, Y.; Xia, L.; Guo, Y.; Zhou, Q. Structural Basis for the Recognition of SARS-CoV-2
4 by Full-Length Human ACE2. *Science* **2020**, *367* (6485), 1444–1448.
5 <https://doi.org/10.1126/science.abb2762>.
- 6 (9) Ortega, J. T.; Serrano, M. L.; Pujol, F. H.; Rangel, H. R. Role of Changes in Sars-Cov-2 Spike Protein in
7 the Interaction With the Human Ace2 Receptor: An in Silico Analysis. *EXCLI J.* **2020**, *19*, 410–417.
- 8 (10) Baig, A. M.; Khaleeq, A.; Ali, U.; Syeda, H. Evidence of the COVID-19 Virus Targeting the CNS: Tissue
9 Distribution, Host-Virus Interaction, and Proposed Neurotropic Mechanisms. *ACS Chem. Neurosci.*
10 **2020**, *11* (7), 995–998. <https://doi.org/10.1021/acscemneuro.0c00122>.
- 11 (11) Doobay, M. F.; Talman, L. S.; Obr, T. D.; Tian, X.; Davisson, R. L.; Lazartigues, E. Differential
12 Expression of Neuronal ACE2 in Transgenic Mice with Overexpression of the Brain Renin-
13 Angiotensin System. *Am. J. Physiol. Regul. Integr. Comp. Physiol.* **2007**, *292* (1), R373–381.
14 <https://doi.org/10.1152/ajpregu.00292.2006>.
- 15 (12) Gowrisankar, Y. V.; Clark, M. A. Angiotensin II Regulation of Angiotensin-Converting Enzymes in
16 Spontaneously Hypertensive Rat Primary Astrocyte Cultures. *J. Neurochem.* **2016**, *138* (1), 74–85.
17 <https://doi.org/10.1111/jnc.13641>.
- 18 (13) Xia, H.; Lazartigues, E. Angiotensin-Converting Enzyme 2: Central Regulator for Cardiovascular
19 Function. *Curr. Hypertens. Rep.* **2010**, *12* (3), 170–175. <https://doi.org/10.1007/s11906-010-0105-7>.
- 20 (14) Wrapp, D.; Wang, N.; Corbett, K. S.; Goldsmith, J. A.; Hsieh, C. L.; Abiona, O.; Graham, B. S.;
21 McLellan, J. S. Cryo-EM Structure of the 2019-NCoV Spike in the Prefusion Conformation. *Science*
22 **2020**, *367* (6483), 1260–1263.
- 23 (15) Li, Y.-C.; Bai, W.-Z.; Hashikawa, T. The Neuroinvasive Potential of SARS-CoV2 May Play a Role in the
24 Respiratory Failure of COVID-19 Patients. *J. Med. Virol.* **2020**. <https://doi.org/10.1002/jmv.25728>.
- 25 (16) Mao, L.; Wang, M.; Chen, S.; He, Q.; Chang, J.; Hong, C.; Zhou, Y.; Wang, D.; Li, Y.; Jin, H.; Hu, B.
26 Neurological Manifestations of Hospitalized Patients with COVID-19 in Wuhan, China: A
27 Retrospective Case Series Study. *medRxiv* **2020**, 2020.02.22.20026500.
28 <https://doi.org/10.1101/2020.02.22.20026500>.
- 29 (17) Filatov, A.; Sharma, P.; Hindi, F.; Espinosa, P. S.; A, F.; P, S.; F, H.; S, E. P. Neurological Complications
30 of Coronavirus Disease (COVID-19): Encephalopathy. *Cureus J. Med. Sci.* **2020**, *12* (3).
31 <https://doi.org/10.7759/cureus.7352>.
- 32 (18) Poyiadji, N.; Shahin, G.; Noujaim, D.; Stone, M.; Patel, S.; Griffith, B. COVID-19–Associated Acute
33 Hemorrhagic Necrotizing Encephalopathy: CT and MRI Features. *Radiology* **2020**,
34 201187. <https://doi.org/10.1148/radiol.2020201187>.
- 35 (19) Rossi, A. Imaging of Acute Disseminated Encephalomyelitis. *Neuroimaging Clin. N. Am.* **2008**, *18* (1),
36 149–161. <https://doi.org/10.1016/j.nic.2007.12.007>.
- 37 (20) Hung, E. C. W.; Chim, S. S. C.; Chan, P. K. S.; Tong, Y. K.; Ng, E. K. O.; Chiu, R. W. K.; Leung, C.-B.;
38 Sung, J. J. Y.; Tam, J. S.; Lo, Y. M. D. Detection of SARS Coronavirus RNA in the Cerebrospinal Fluid of
39 a Patient with Severe Acute Respiratory Syndrome. *Clin. Chem.* **2003**, *49* (12), 2108–2109.
40 <https://doi.org/10.1373/clinchem.2003.025437>.
- 41 (21) He, L.; Ding, Y.; Che, X.; Zhang, Q.; Huang, Z.; Wang, H.; Shen, H.; Li, Z.; Cai, J.; Zhang, J.; Geng, J.; Li,
42 X.; Zhang, W.; Han, H.; Kang, W.; Yang, L.; Lu, Y. [Expression of the monoclonal antibody against
43 nucleocapsid antigen of SARS-associated coronavirus in autopsy tissues from SARS patients]. *1 Jun*
44 *Yi Xue Xue Bao Acad. J. First Med. Coll. PLA* **2003**, *23* (11), 1128–1130.
- 45 (22) Ding, Y.; He, L.; Zhang, Q.; Huang, Z.; Che, X.; Hou, J.; Wang, H.; Shen, H.; Qiu, L.; Li, Z.; Geng, J.; Cai,
46 J.; Han, H.; Li, X.; Kang, W.; Weng, D.; Liang, P.; Jiang, S. Organ Distribution of Severe Acute
47 Respiratory Syndrome (SARS) Associated Coronavirus (SARS-CoV) in SARS Patients: Implications for
48 Pathogenesis and Virus Transmission Pathways. *J. Pathol.* **2004**, *203* (2), 622–630.
49 <https://doi.org/10.1002/path.1560>.
- 50
51
52
53
54
55
56
57
58
59
60

- 1
2
3 (23) Gu, J.; Gong, E.; Zhang, B.; Zheng, J.; Gao, Z.; Zhong, Y.; Zou, W.; Zhan, J.; Wang, S.; Xie, Z.; Zhuang,
4 H.; Wu, B.; Zhong, H.; Shao, H.; Fang, W.; Gao, D.; Pei, F.; Li, X.; He, Z.; Xu, D.; Shi, X.; Anderson, V.
5 M.; Leong, A. S.-Y. Multiple Organ Infection and the Pathogenesis of SARS. *J. Exp. Med.* **2005**, *202*
6 (3), 415–424. <https://doi.org/10.1084/jem.20050828>.
- 7
8 (24) Xu, J.; Zhong, S.; Liu, J.; Li, L.; Li, Y.; Wu, X.; Li, Z.; Deng, P.; Zhang, J.; Zhong, N.; Ding, Y.; Jiang, Y.
9 Detection of Severe Acute Respiratory Syndrome Coronavirus in the Brain: Potential Role of the
10 Chemokine Mig in Pathogenesis. *Clin. Infect. Dis. Off. Publ. Infect. Dis. Soc. Am.* **2005**, *41* (8), 1089–
11 1096. <https://doi.org/10.1086/444461>.
- 12 (25) Jaimes, J. A.; Andre, N. M.; Millet, J. K.; Whittaker, G. R. Structural Modeling of 2019–Novel
13 Coronavirus (NCoV) Spike Protein Reveals a Proteolytically-Sensitive Activation Loop as a
14 Distinguishing Feature Compared to SARS-CoV and Related SARS-like Coronaviruses. **2020**, No.
15 February.
- 16 (26) Baig, A. M.; Khaleeq, A.; Ali, U.; Syeda, H. Evidence of the COVID-19 Virus Targeting the CNS: Tissue
17 Distribution, Host–Virus Interaction, and Proposed Neurotropic Mechanisms. *ACS Chem. Neurosci.*
18 **2020**, 0–3.
- 19 (27) Robson, B. COVID-19 Coronavirus Spike Protein Analysis for Synthetic Vaccines, a Peptidomimetic
20 Antagonist, and Therapeutic Drugs, and Analysis of a Proposed Achilles’ Heel Conserved Region to
21 Minimize Probability of Escape Mutations and Drug Resistance. *Comput. Biol. Med.* **2020**, *121*,
22 103749. <https://doi.org/10.1016/j.compbiomed.2020.103749>.
- 23 (28) Bongrand, P. Specific and Nonspecific Interactions in Cell Biology. *J. Dispers. Sci. Technol.* **1998**, *19*
24 (6–7), 963–978.
- 25 (29) Sancini, G.; Gregori, M.; Salvati, E.; Cambianica, I.; Re, F.; Ornaghi, F.; Canovi, M.; Fracasso, C.;
26 Cagnotto, A.; Colombo, M.; Zona, C.; Gobbi, M.; Salmona, M.; La Ferla, B.; Nicotra, F.; Masserini, M.
27 Functionalization with TAT-Peptide Enhances Blood-Brain Barrier Crossing in Vitro of
28 Nanoliposomes Carrying a Curcumin-Derivative to Bind Amyloid- β Peptide. **2013**, *4* (3), 1–8.
29 <https://doi.org/10.4172/2157-7439.1000171>.
- 30 (30) Johansson, H.; Jensen, M. R.; Gesmar, H.; Meier, S.; Vinther, J. M.; Keeler, C.; Hodsdon, M. E.; Led, J. J.
31 Specific and Nonspecific Interactions in Ultraweak Protein-Protein Associations Revealed by
32 Solvent Paramagnetic Relaxation Enhancements. *J. Am. Chem. Soc.* **2014**, *136* (29), 10277–10286.
- 33 (31) Lan, J.; Ge, J.; Yu, J.; Shan, S.; Zhou, H.; Fan, S.; Zhang, Q.; Shi, X.; Wang, Q.; Zhang, L.; Wang, X.
34 Structure of the SARS-CoV-2 Spike Receptor-Binding Domain Bound to the ACE2 Receptor. *Nature*
35 **2020**, *581* (7807), 215–220. <https://doi.org/10.1038/s41586-020-2180-5>.
- 36 (32) Vorbrod, A. W. Demonstration of Anionic Sites on the Luminal and Abluminal Fronts of Endothelial
37 Cells with Poly-L-Lysine-Gold Complex. *J. Histochem. Cytochem. Off. J. Histochem. Soc.* **1987**, *35*
38 (11), 1261–1266. <https://doi.org/10.1177/35.11.3655325>.
- 39 (33) Amin, M.; Sorour, M. K.; Kasry, A. Comparing the Binding Interactions in the Receptor Binding
40 Domains of SARS-CoV-2 and SARS-CoV. *J. Phys. Chem. Lett.* **2020**, *11*, 4897–4900.
41 <https://doi.org/10.1021/acs.jpcclett.0c01064>.
- 42 (34) Wang, Y.; Liu, M.; Gao, J. Enhanced Receptor Binding of SARS-CoV-2 through Networks of
43 Hydrogen-Bonding and Hydrophobic Interactions. *Proc. Natl. Acad. Sci. U. S. A.* **2020**, *117* (25),
44 13967–13974. <https://doi.org/10.1073/pnas.2008209117>.
- 45 (35) Calligari, P.; Bobone, S.; Ricci, G.; Bocedi, A. Molecular Investigation of SARS-CoV-2 Proteins and
46 Their Interactions with Antiviral Drugs. *Viruses* **2020**, *12* (4). <https://doi.org/10.3390/v12040445>.
- 47 (36) Sancini, G.; Dal Magro, R.; Ornaghi, F.; Balducci, C.; Forloni, G.; Gobbi, M.; Salmona, M.; Re, F.
48 Pulmonary Administration of Functionalized Nanoparticles Significantly Reduces Beta-Amyloid in
49 the Brain of an Alzheimer’s Disease Murine Model. *Nano Res.* **2016**, *9* (7), 2190–2201.
50 <https://doi.org/10.1007/s12274-016-1108-8>.
- 51
52
53
54
55
56
57
58
59
60

- 1
2
3 (37) Steardo, L.; Steardo, L.; Zorec, R.; Verkhatsky, A. Neuroinfection May Contribute to
4 Pathophysiology and Clinical Manifestations of COVID-19. *Acta Physiol. Oxf. Engl.* **2020**, e13473.
5 <https://doi.org/10.1111/apha.13473>.
- 6 (38) Dijkman, R.; Jebbink, M. F.; Deijs, M.; Milewska, A.; Pyrc, K.; Buelow, E.; van der Bijl, A.; van der
7 Hoek, L. Replication-Dependent Downregulation of Cellular Angiotensin-Converting Enzyme 2
8 Protein Expression by Human Coronavirus NL63. *J. Gen. Virol.* **2012**, *93* (Pt 9), 1924–1929.
9 <https://doi.org/10.1099/vir.0.043919-0>.
- 10 (39) Kuba, K.; Imai, Y.; Rao, S.; Gao, H.; Guo, F.; Guan, B.; Huan, Y.; Yang, P.; Zhang, Y.; Deng, W.; Bao, L.;
11 Zhang, B.; Liu, G.; Wang, Z.; Chappell, M.; Liu, Y.; Zheng, D.; Leibbrandt, A.; Wada, T.; Slutsky, A. S.;
12 Liu, D.; Qin, C.; Jiang, C.; Penninger, J. M. A Crucial Role of Angiotensin Converting Enzyme 2 (ACE2)
13 in SARS Coronavirus-Induced Lung Injury. *Nat. Med.* **2005**, *11* (8), 875–879.
14 <https://doi.org/10.1038/nm1267>.
- 15 (40) Watkins, J. Preventing a Covid-19 Pandemic. *BMJ* **2020**, *368*, m810.
16 <https://doi.org/10.1136/bmj.m810>.
- 17 (41) Glowacka, I.; Bertram, S.; Herzog, P.; Pfefferle, S.; Steffen, I.; Muench, M. O.; Simmons, G.;
18 Hofmann, H.; Kuri, T.; Weber, F.; Eichler, J.; Drosten, C.; Pöhlmann, S. Differential Downregulation
19 of ACE2 by the Spike Proteins of Severe Acute Respiratory Syndrome Coronavirus and Human
20 Coronavirus NL63. *J. Virol.* **2010**, *84* (2), 1198–1205. <https://doi.org/10.1128/JVI.01248-09>.
- 21 (42) Terrence, C. F.; Rao, G. R.; Perper, J. A. Neurogenic Pulmonary Edema in Unexpected, Unexplained
22 Death of Epileptic Patients. *Ann. Neurol.* **1981**, *9* (5), 458–464.
23 <https://doi.org/10.1002/ana.410090508>.
- 24 (43) Šedý, J.; Kuneš, J.; Zicha, J. Pathogenetic Mechanisms of Neurogenic Pulmonary Edema. *J.*
25 *Neurotrauma* **2015**, *32* (15), 1135–1145. <https://doi.org/10.1089/neu.2014.3609>.
- 26 (44) Karimi, N.; Sharifi Razavi, A.; Rouhani, N. Frequent Convulsive Seizures in an Adult Patient with
27 COVID-19: A Case Report <http://ircmj.com/en/articles/102828.html> (accessed Apr 22, 2020).
28 <https://doi.org/10.5812/ircmj.102828>.
- 29 (45) Libbey, J. E.; Fujinami, R. S. Neurotropic Viral Infections Leading to Epilepsy: Focus on Theiler's
30 Murine Encephalomyelitis Virus. *Future Virol.* **2011**, *6* (11), 1339–1350.
31 <https://doi.org/10.2217/fvl.11.107>.
- 32 (46) Huang, C.; Wang, Y.; Li, X.; Ren, L.; Zhao, J.; Hu, Y.; Zhang, L.; Fan, G.; Xu, J.; Gu, X.; Cheng, Z.; Yu, T.;
33 Xia, J.; Wei, Y.; Wu, W.; Xie, X.; Yin, W.; Li, H.; Liu, M.; Xiao, Y.; Gao, H.; Guo, L.; Xie, J.; Wang, G.;
34 Jiang, R.; Gao, Z.; Jin, Q.; Wang, J.; Cao, B. Clinical Features of Patients Infected with 2019 Novel
35 Coronavirus in Wuhan, China. *Lancet Lond. Engl.* **2020**, *395* (10223), 497–506.
36 [https://doi.org/10.1016/S0140-6736\(20\)30183-5](https://doi.org/10.1016/S0140-6736(20)30183-5).
- 37 (47) Zhao, M. Cytokine Storm and Immunomodulatory Therapy in COVID-19: Role of Chloroquine and
38 Anti-IL-6 Monoclonal Antibodies. *Int. J. Antimicrob. Agents* **2020**.
39 <https://doi.org/10.1016/j.ijantimicag.2020.105982>.
- 40 (48) Singhi, P. Infectious Causes of Seizures and Epilepsy in the Developing World. *Dev. Med. Child*
41 *Neurol.* **2011**, *53* (7), 600–609. <https://doi.org/10.1111/j.1469-8749.2011.03928.x>.
- 42 (49) Libbey, J. E.; Kennett, N. J.; Wilcox, K. S.; White, H. S.; Fujinami, R. S. Interleukin-6, Produced by
43 Resident Cells of the Central Nervous System and Infiltrating Cells, Contributes to the Development
44 of Seizures Following Viral Infection. *J. Virol.* **2011**, *85* (14), 6913–6922.
45 <https://doi.org/10.1128/JVI.00458-11>.
- 46 (50) Libbey, J. E.; Kirkman, N. J.; Smith, M. C. P.; Tanaka, T.; Wilcox, K. S.; White, H. S.; Fujinami, R. S.
47 Seizures Following Picornavirus Infection. *Epilepsia* **2008**, *49* (6), 1066–1074.
48 <https://doi.org/10.1111/j.1528-1167.2008.01535.x>.
- 49 (51) Ye, M.; Ren, Y.; Lv, T. Encephalitis as a Clinical Manifestation of COVID-19. *Brain. Behav. Immun.*
50 **2020**. <https://doi.org/10.1016/j.bbi.2020.04.017>.
- 51
52
53
54
55
56
57
58
59
60

- 1
2
3 (52) Hummel, T.; Whitcroft, K. L.; Andrews, P.; Altundag, A.; Cinghi, C.; Costanzo, R. M.; Damm, M.;
4 Frasnelli, J.; Gudziol, H.; Gupta, N.; Haehner, A.; Holbrook, E.; Hong, S. C.; Hornung, D.; Hüttenbrink,
5 K. B.; Kamel, R.; Kobayashi, M.; Konstantinidis, I.; Landis, B. N.; Leopold, D. A.; Macchi, A.; Miwa, T.;
6 Moesges, R.; Mullol, J.; Mueller, C. A.; Ottaviano, G.; Passali, G. C.; Philpott, C.; Pinto, J. M.;
7 Ramakrishnan, V. J.; Rombaux, P.; Roth, Y.; Schlosser, R. A.; Shu, B.; Soler, G.; Stjärne, P.; Stuck, B.
8 A.; Vodicka, J.; Welge-Luessen, A. Position Paper on Olfactory Dysfunction. *Rhinology* **2016**, *56* (1),
9 1–30. <https://doi.org/10.4193/Rhin16.248>.
- 10 (53) Welge-Lüssen, A. Re-Establishment of Olfactory and Taste Functions. *GMS Curr. Top.*
11 *Otorhinolaryngol. Head Neck Surg.* **2005**, *4*.
- 12 (54) Giacomelli, A.; Pezzati, L.; Conti, F.; Bernacchia, D.; Siano, M.; Oreni, L.; Rusconi, S.; Gervasoni, C.;
13 Ridolfo, A. L.; Rizzardini, G.; Antinori, S.; Galli, M. Self-Reported Olfactory and Taste Disorders in
14 SARS-CoV-2 Patients: A Cross-Sectional Study. *Clin. Infect. Dis. Off. Publ. Infect. Dis. Soc. Am.* **2020**.
15 <https://doi.org/10.1093/cid/ciaa330>.
- 16 (55) Bagheri, S. H. R.; Asghari, A. M.; Farhadi, M.; Shamshiri, A. R.; Kabir, A.; Kamrava, S. K.; Jalessi, M.;
17 Mohebbi, A.; Alizadeh, R.; Honarmand, A. A.; Ghalehbaghi, B.; Salimi, A. Coincidence of COVID-19
18 Epidemic and Olfactory Dysfunction Outbreak. *medRxiv* **2020**, 2020.03.23.20041889.
19 <https://doi.org/10.1101/2020.03.23.20041889>.
- 20 (56) Lechien, J. R.; Chiesa-Estomba, C. M.; De Siati, D. R.; Horoi, M.; Le Bon, S. D.; Rodriguez, A.;
21 Dequanter, D.; Blecic, S.; El Afia, F.; Distinguin, L.; Chekkoury-Idrissi, Y.; Hans, S.; Delgado, I. L.;
22 Calvo-Henriquez, C.; Lavigne, P.; Falanga, C.; Barillari, M. R.; Cammaroto, G.; Khalife, M.; Leich, P.;
23 Souchay, C.; Rossi, C.; Journe, F.; Hsieh, J.; Edjlali, M.; Carlier, R.; Ris, L.; Lovato, A.; De Filippis, C.;
24 Coppee, F.; Fakhry, N.; Ayad, T.; Saussez, S. Olfactory and Gustatory Dysfunctions as a Clinical
25 Presentation of Mild-to-Moderate Forms of the Coronavirus Disease (COVID-19): A Multicenter
26 European Study. *Eur. Arch. Otorhinolaryngol.* **2020**. <https://doi.org/10.1007/s00405-020-05965-1>.
- 27 (57) Perlman, S.; Evans, G.; Afifi, A. Effect of Olfactory Bulb Ablation on Spread of a Neurotropic
28 Coronavirus into the Mouse Brain. *J. Exp. Med.* **1990**, *172* (4), 1127–1132.
29 <https://doi.org/10.1084/jem.172.4.1127>.
- 30 (58) Mohammed, A. K.; Magnusson, O.; Maehlen, J.; Fonnum, F.; Norrby, E.; Schultzberg, M.;
31 Kristensson, K. Behavioural Deficits and Serotonin Depletion in Adult Rats after Transient Infant
32 Nasal Viral Infection. *Neuroscience* **1990**, *35* (2), 355–363. [https://doi.org/10.1016/0306-](https://doi.org/10.1016/0306-4522(90)90089-M)
33 [4522\(90\)90089-M](https://doi.org/10.1016/0306-4522(90)90089-M).
- 34 (59) Seiden, A. M. Postviral Olfactory Loss. *Otolaryngol. Clin. North Am.* **2004**, *37* (6), 1159–1166.
35 <https://doi.org/10.1016/j.otc.2004.06.007>.
- 36 (60) Dalton, P. Olfaction and Anosmia in Rhinosinusitis. *Curr. Allergy Asthma Rep.* **2004**, *4* (3), 230–236.
37 <https://doi.org/10.1007/s11882-004-0031-3>.
- 38 (61) Hummel, T.; Landis, B. N.; Hüttenbrink, K.-B. Smell and Taste Disorders. *GMS Curr. Top.*
39 *Otorhinolaryngol. Head Neck Surg.* **2012**, *10*. <https://doi.org/10.3205/cto000077>.
- 40 (62) Altschul, S. F.; Gish, W.; Miller, W.; Myers, E. W.; Lipman, D. J. Basic Local Alignment Search Tool. *J.*
41 *Mol. Biol.* **1990**, *215* (3), 403–410. [https://doi.org/10.1016/S0022-2836\(05\)80360-2](https://doi.org/10.1016/S0022-2836(05)80360-2).
- 42 (63) Henikoff, S.; Henikoff, J. G. Amino Acid Substitution Matrices from Protein Blocks. *Proc. Natl. Acad.*
43 *Sci. U. S. A.* **1992**, *89* (22), 10915–10919.
- 44 (64) Abagyan, R. A.; Batalov, S. Do Aligned Sequences Share the Same Fold? *J. Mol. Biol.* **1997**, *273* (1),
45 355–368.
- 46 (65) Molsoft L.L.C.: ICM-Browser http://www.molsoft.com/icm_browser.html (accessed Jul 1, 2020).
- 47 (66) RStudio Team. RStudio: Integrated Development for R. Boston, MA 2015.
- 48 (67) Fiser, A.; Šali, A. MODELLER: Generation and Refinement of Homology-Based Protein Structure
49 Models. *Methods Enzymol.* **2003**, *374*, 461–491.
- 50 (68) RCSB PDB: Homepage <https://www.rcsb.org/> (accessed Apr 7, 2020).
- 51
52
53
54
55
56
57
58
59
60

- 1
2
3 (69) Pettersen, E. F.; Goddard, T. D.; Huang, C. C.; Couch, G. S.; Greenblatt, D. M.; Meng, E. C.; Ferrin, T.
4 E. UCSF Chimera - A Visualization System for Exploratory Research and Analysis. *J. Comput. Chem.*
5 **2004**, *25* (13), 1605–1612.
6 (70) Baker, N. A.; Sept, D.; Joseph, S.; Holst, M. J.; McCammon, J. A. Electrostatics of Nanosystems:
7 Application to Microtubules and the Ribosome. *Proc. Natl. Acad. Sci. U. S. A.* **2001**, *98* (18), 10037–
8 10041.
9 (71) DELANO, W. L. The PyMOL Molecular Graphics System. 2002.
10 (72) Lerner, M. G.; Carlson, H. A. APBS Plugin for PyMOL. Arbor: University of Michigan 2006.
11 (73) Massova, I.; Kollman, P. A. Combined Molecular Mechanical and Continuum Solvent Approach
12 (MM- PBSA/GBSA) to Predict Ligand Binding. *Perspect. Drug Discov. Des.* **2000**, *18* (i), 113–135.
13 (74) Kumari, R.; Kumar, R.; Lynn, A. G-Mmpbsa -A GROMACS Tool for High-Throughput MM-PBSA
14 Calculations. *J. Chem. Inf. Model.* **2014**, *54* (7), 1951–1962.
15 (75) Ramos, R. M.; Moreira, I. S. Computational Alanine Scanning Mutagenesis-An Improved
16 Methodological Approach for Protein-DNA Complexes. *J. Chem. Theory Comput.* **2013**, *9* (9), 4243–
17 4256. <https://doi.org/10.1021/ct400387r>.
18 (76) Berendsen, H. J. C.; van der Spoel, D.; van Drunen, R. GROMACS: A Message-Passing Parallel
19 Molecular Dynamics Implementation. *Comput. Phys. Commun.* **1995**, *91* (1–3), 43–56.
20
21
22
23
24
25
26
27
28
29
30
31
32
33
34
35
36
37
38
39
40
41
42
43
44
45
46
47
48
49
50
51
52
53
54
55
56
57
58
59
60

Table 1. Number of each residue present in the S protein of SARS-CoV-2 and SARS-CoV. The different residues are represented with the one letter code. Positively charged residues are highlighted in light blue and negatively charged residues in light red.

Residuo	SARS-CoV-2	SARS-CoV
A	79	84
R	42	39
N	88	81
D	62	73
C	40	39
Q	62	55
E	48	42
G	82	79
H	17	15
I	76	78
L	108	99
K	61	60
M	14	20
F	77	83
P	58	57
S	99	96
T	97	99
W	12	11
Y	54	54
V	97	91

Figure Legends:

1
2
3
4
5
6
7
8
9
10
11
12
13
14
15
16
17
18
19
20
21
22
23
24
25
26
27
28
29
30
31
32
33
34
35
36
37
38
39
40
41
42
43
44
45
46
47
48
49
50
51
52
53
54
55
56
57
58
59
60

1. **Sequence alignment of SARS-CoV-2 and SARS-CoV S protein.** Conserved residues are labelled in dark green, same residues in lighter green and residues with similar properties in yellow.

2. **Electrostatic potential of Spike protein in SARS-CoV-2 vs SARS-CoV.** Electrostatic potential of (A) SARS-CoV-2 and (B) SARS-CoV S protein in the (1) close and (2) open conformations mapped onto their molecular surface. This region represents the top side of the protein where the RBD is located, thus, the opposite side to the one that is attached to the surface of the virus. The negative electrostatic potential is shown in red, the neutral in white, and the positive in blue. Values ranging from $-kT/e$ (red) to $+kT/e$ (blue).

3. **Electrostatic potential of (A) SARS-CoV-2 (PDB ID GLZG) and (B) SARS-CoV (PDB ID 6ACJ, A) S protein RBD section** mapped onto its molecular surface when in complex with human ACE2 receptor (transparent green). The negative electrostatic potential is shown in red, the neutral in white, and the positive in blue. Values ranging from $-kT/e$ (red) to $+kT/e$ (blue).

4. **Electrostatic potential of human ACE2 receptor.** Electrostatic potential of human ACE2 receptor mapped onto its molecular surface when in complex with SARS-CoV-2 (cyan) (PDB ID GLZG) shown from different perspectives. The negative electrostatic potential is shown in red, the neutral in white, and the positive in blue. Values ranging from $-kT/e$ (red) to $+kT/e$ (blue).

5. **Brain and lung crosstalk in the COVID-19 infection.** COVID-19 employs ACE2 as receptor for viral cell entry and induction of lung injury through increasing the immune system cytokines. It can downregulate the central ACE2 protein expression; inhibition of ACE2 activity, reduces the sensitivity of the baroreceptor reflex control of heart rate as well as increase in sympathetic tone which eventually resulting in the blood pressure elevation and cardiac dysfunction. In addition, concerning the neuroprotective property of ACE2, its downregulation may disturb the balance of neurotoxicity/neuroprotection inside the brain. Increasing of inflammatory cytokines during lung injury, hypoxemia and elevation of sympathetic tone through ACE2 downregulation leads to CNS hyper-activation which might play a crucial role in etiopathogenesis of neurogenic pulmonary edema which may play a role in the COVID-19 pulmonary complications in patients. ACE2: Angiotensin-Converting Enzyme 2, NPE: Neurogenic Pulmonary Edema, NP: Neuroprotection, NT: Neurotoxicity.


```

SARS_CoV_2 1 MVEVILVLPVSV---SQVNLITRTQLPAAFNSTP--RGVYVQKVFSSVLSHTQQLPFFSNVTFPHALIVSGNTGKRDONVLPVENDGVFEA
SARS_CoV 1 MEIIEILPITLTSGLDLDKRTTFDDVQ--AATVQHTSSMRGVYVFOIERSOTLYLQQLLLETFYSNVTCQETIN-----HTGQVILPFDGILIEA

SARS_CoV_2 94 STEKSNITIRGIIIGTLLDSEYQLLIVNNAIVVIVKVEIQPQNDNDFLQVYRKNNSMBSSEFRVYSSAMNCTFSEVSPQFLADLEGQCNQNFQLEEF
SARS_CoV 91 ATEKSNVIRGIVGSETPNNKCGSVIISNITNVIYIAENRILQVDFPQV---SEKNGTQYRTHIFQNAFPTGTEIISDAELIDVSECSSEKFLKSEF

SARS_CoV_2 193 VFKNIDGYFKIISKRTINLIVHDLQCSALELVDLHIGINIFRQTLALHRSYLTGDSSSGCTAGAAAIVYGLQDPTFLKLNENGTITDAVDC
SARS_CoV 186 VFKNIDGFLYVKGVQIDVYHDLISGENTLKIIFKLELGININERAILTA---FSQAQDI--HCTSAAAIFVGLKPTTFLKLNENGTITDAVDC

SARS_CoV_2 292 ALDLESEKTKLSEIVKEGIQVTSNFRVQTEISIVRFRNITNLCRQGVFNATRFASVYAMRKRKISNGVADSVLNSASFTFKCGVSPFKLNDL
SARS_CoV 279 SQNLELAEIKSVKSEIIDKGIQVTSNFRVSGDQVYRFRNITNLCRQGVFNATRFASVYAMRKRKISNGVADSVLNSASFTFKCGVSPFKLNDL

SARS_CoV_2 391 RFTNVYADSEVIRGDEVRQIAPQDQKIDAEYKLEDDTCEVIAMNNSLSEKVCNNTLFLFKSNKKEFERDITETIYQAGSTINQVRCFQK
SARS_CoV 378 RFTNVYADSEVIRGDEVRQIAPQDQKIDAEYKLEDDTCEVIAMNNSLSEKVCNNTLFLFKSNKKEFERDITETIYQAGSTINQVRCFQK

SARS_CoV_2 490 FTEQSGIQPTNGVCIQVFRVVVLSPELLNATVCGEKKSTNENKRVNPNFNGLTGTVLTSNKKELFQQGRDIADTDAVRDQTEILIDIT
SARS_CoV 476 NEMLDGCTTTTIGIQVFRVVVLSPELLNATVCGEKKSTNENKRVNPNFNGLTGTVLTSNKKELFQQGRDRVSDPTDSVRDEKTSRILDIS

SARS_CoV_2 589 RSEKGGVSVITKQNTENQVAVLQDQVQTEVPVAIHADQLTFRVYVSTGSRVYQTAGELIGAEVNNSEEDISIGAGICASVQVQVNSFRPAREV
SARS_CoV 575 RSEKGGVSVITKQNTENQVAVLQDQVQTEVPVAIHADQLTFRVYVSTGSRVYQTAGELIGAEVNNSEEDISIGAGICASVQVQVNSFRPAREV

SARS_CoV_2 688 AQGSIIVANMELGDRVAVNNSLAIETNITIVTTEILLVNNITVSDVTEMLQDSTTEHLLQCGFTQGRALGLIIVQDQNTQVFAQV
SARS_CoV 670 RQKSIIVANMELGDRVAVNNSLAIETNITIVTTEILLVNNITVSDVTEMLQDSTTEHLLQCGFTQGRALGLIIVQDQNTQVFAQV

SARS_CoV_2 787 QIIRKTPIDKGGNFQILLQSKSKRSIEDLLNRYVLADAGIKVQDGLDIAARDLCAQKFNGLTVLPLITDQMIQATYALLAGTITQ
SARS_CoV 769 QIIRKTPIDKGGNFQILLQSKSKRSIEDLLNRYVLADAGIKVQDGLDIAARDLCAQKFNGLTVLPLITDQMIQATYALLAGTITQ

SARS_CoV_2 866 RTGAGAAQLIFAMQGAIRFNGIGVYQVLYENQELIANQNSAIGKIQDELSTASALGKLVQVNNQAQALNVLKQLSSNCAISSVLDLISRL
SARS_CoV 868 RTGAGAAQLIFAMQGAIRFNGIGVYQVLYENQELIANQNSAIGKIQDELSTASALGKLVQVNNQAQALNVLKQLSSNCAISSVLDLISRL

SARS_CoV_2 985 DKVBARVQIDRLITGRQLQFTVYQQLIRAAIRASANLAATMSSEVLDQSKRVDFQSGVHLSHFQGRHGVVFLVTVFAQRNFTTAAIAR
SARS_CoV 967 DKVBARVQIDRLITGRQLQFTVYQQLIRAAIRASANLAATMSSEVLDQSKRVDFQSGVHLSHFQGRHGVVFLVTVFAQRNFTTAAIAR

SARS_CoV_2 1084DKGANFREGVIVNGTHFVYQNFYEQIITTDNTVSGNDVVGIVNNTVYDILQDELDSKKELDKIFKNHITSEVDLGDLSGINASVYVNIQK
SARS_CoV 1066DKGANFREGVIVNGTHFVYQNFYEQIITTDNTVSGNDVVGIVNNTVYDILQDELDSKKELDKIFKNHITSEVDLGDLSGINASVYVNIQK

SARS_CoV_2 1183YDRLNKVAKNNSLIDLQELQKTEQIFKFWYIHLGFIAGLIAVHVYIIMLCMTSCCSSEKGCSESGSCKEDEDSEVPLKGVLEIT
SARS_CoV 1165YDRLNKVAKNNSLIDLQELQKTEQIFKFWYIHLGFIAGLIAVHVYIIMLCMTSCCSSEKGCSESGSCKEDEDSEVPLKGVLEIT

```

Figure 1

338x190mm (96 x 96 DPI)

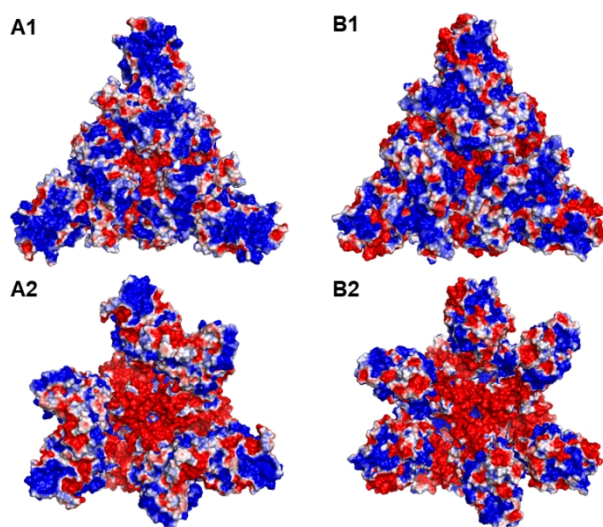


Figure 2

338x190mm (96 x 96 DPI)

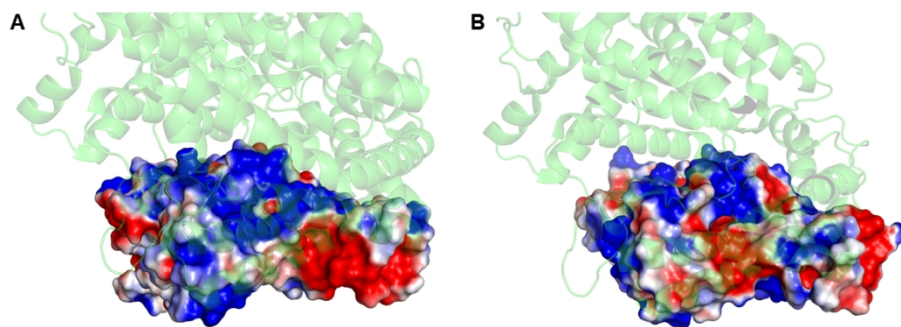


Figure 3

338x190mm (96 x 96 DPI)

1
2
3
4
5
6
7
8
9
10
11
12
13
14
15
16
17
18
19
20
21
22
23
24
25
26
27
28
29
30
31
32
33
34
35
36
37
38
39
40
41
42
43
44
45
46
47
48
49
50
51
52
53
54
55
56
57
58
59
60

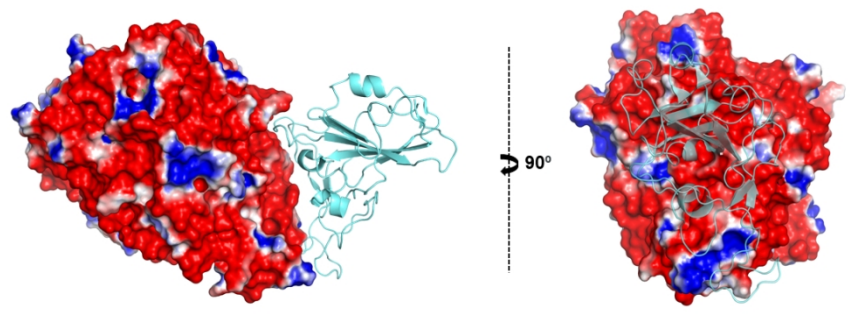


Figure 4

338x190mm (96 x 96 DPI)

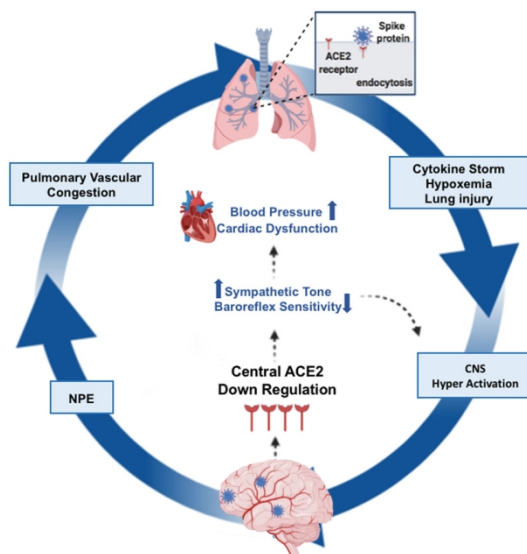


Figure 5